Assignment SC42095: VTOL Aircraft

by

Lorenzo Terenzi 4465156

Contents

Introduction

In this assignment, we designed several controllers, both discrete and continuous, for a vertical take-off and landing aircraft. In particular, the vertical take-off aircraft (Möller International USA) has the following transfer function between input (position of the motors) and the output (altitude, vertical position):

$$G = \frac{1}{s^2(s^2 + s + 4)} \tag{1}$$

The report is structured is structured as follows. In chapter 1 we designed two continuous controllers, one for servo-tracking and the other tuned for disturbance rejection.

The two controllers are discretized in chapter 2 by appropriately choosing a discretization scheme. Furthermore in chapter 2 we designed a pole placement controller and equipped it with an observer to output-feedback controller. Furthermore, we designed a digital LQR controller for reference tracking.

In chapter 3 we revised the design of the controllers to make sure that the output of the controllers was in magnitude below 2.5 to avoid saturation of the actuators. At the end of the chapter integral action was introduced as a way to generate a robust reference tracking state feedback system.

In chapter 4 we analysed the effects of delays in the control system and redesigned them to meet the original requirements.

1 Continuous time control

In this chapter, we address the design of a continuous time controller for a SISO system first for set-point tracking and then for disturbance rejection

1.1. Set-point tracking

The design of the controller was directed by the following requirements:

1. minimal settling-time
2. overshoot < 5 %
3. No steady-state error

The open loop system in response to a step input is shown in **??** and it's clearly not stable. The instability is caused by the two poles at the origin, the other two poles are located at $-0.5 \pm 1.93i$. To start designing the controller we first examined the frequency response of the system which can be seen in the bode plot in **??**.

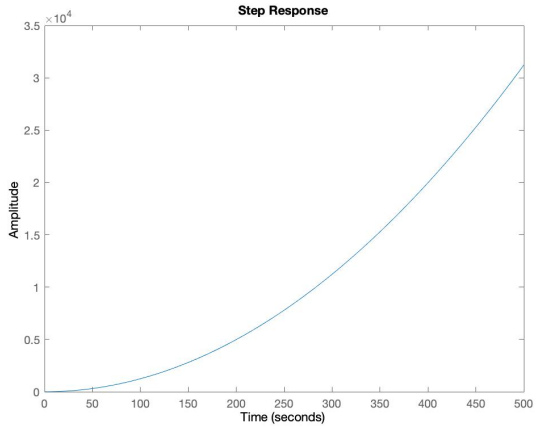

Figure 1.1: Open loop response to a step input

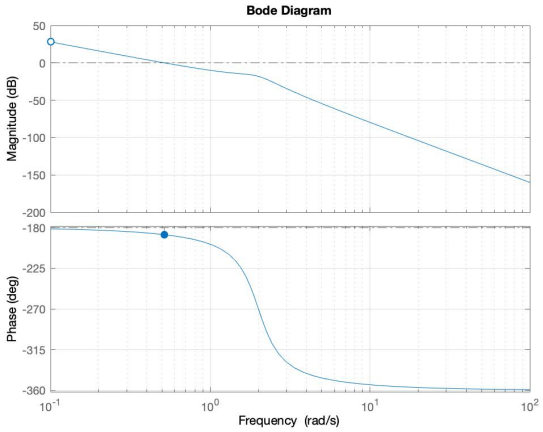

Figure 1.2: Bode plot of open loop system

The system response argument starts with 180° of phase and then decreases to 360° this is reflected as well in the magnitude plot where we observe a slope of 40 dB/decade until 2 rad/sec and then of 80 dB/decade. To have a positive phase margin we have to add lead in the system, this can be done by designing a feedback loop with a derivative controller. The feedback loop structure is shown in **??** where C is the controller. For proportional control, we choose C equal to

$$C = ks = 1.7s \tag{1.1}$$

The first zero was set at the origin to reshape the root locus since now one of the two poles at zero will tend on the towards infinity in the negative real axis. The root loci for the original and modified system can be seen in Figure 1.3 and Figure 1.4.

The gain was chosen to minimise the settling time and to comply with the overshoot requirement. The step response and the new Bode plots can be seen in Figure 1.5 and Figure 1.6.

We can see that there are still some not well-damped oscillations in the response. To reduce the gain of the system at those frequencies we introduced a lag term, which also works as a low pass filter for the different term to avoid

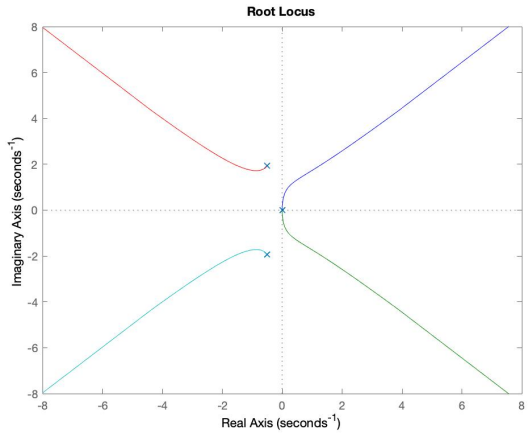

Figure 1.3: Original system's root locus

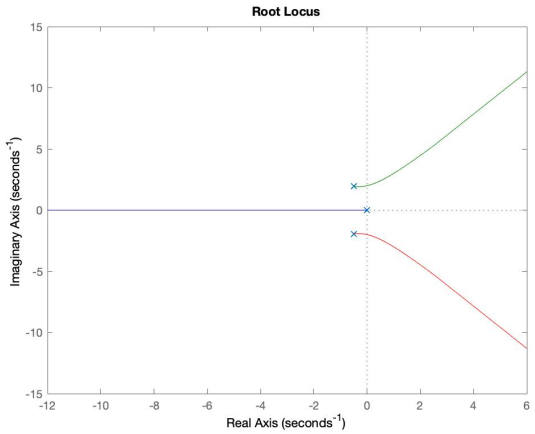

Figure 1.4: Root locus of the plant with the derivative controller

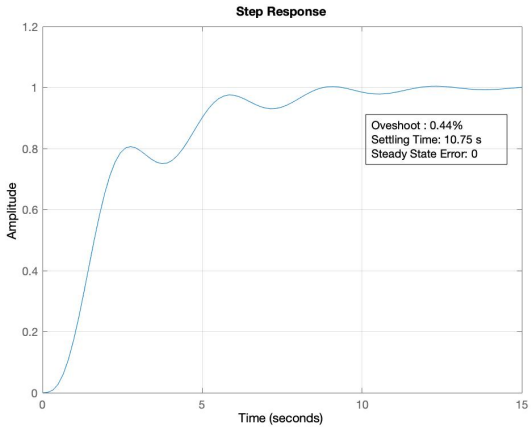

Figure 1.5: Feedback system with derivative controller response to a step input

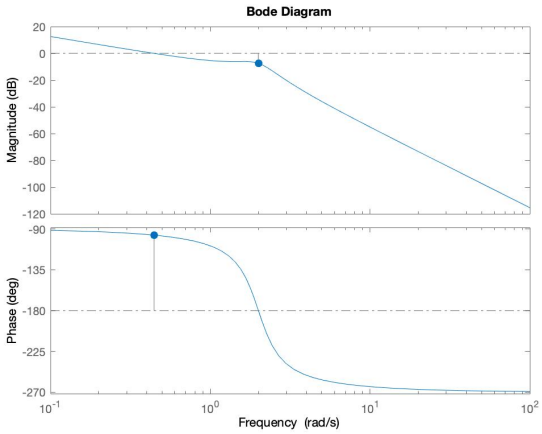

Figure 1.6: Bode plot of the system with derivative controller

performance deterioration due to the presence of noise. The controller C now has the form

$$C = \frac{ks}{1 + s/\omega_i} = \frac{1.54s}{1 + 0.9s} \tag{1.2}$$

ω_1 was chosen to reduce the oscillations that delay the settling time while the gain make the system respond faster. The new step responses and Bode plots are shown in Figure 1.7 and Figure 1.8. The response with the current controller has the following characteristics: overshoot of 1.93 %, no steady state error and a settling time $t_s = 5.686$ sec.

The settling time is still relatively long, but if we increase the cross over frequency w_c the system can respond faster. This implies though that the system is more susceptible to noise and expensive equipment might be needed to actually realize the controller. To increase the cross-over frequency and at the same time add phase we use a lead compensator. For the current system, we need a second order compensator, its numerator is chosen to cancel out the oscillatory behaviours of the system and reduce overshoot. The settling time can be traded off w.r.t the pole positions in the denominator of the transfer function. We set the poles of the compensator at -1000, which might not be fully feasible in practice but we still use it to minimize the settling time. The final form of the controller is

$$C = K * \frac{k_p + 2s}{1 + 0.01s} \frac{s^2 + s + 4}{(1 + s * T)^2} = 20 \frac{0.1 + 2s}{1 + 0.01s} \frac{s^2 + s + 4}{(1 + 0.001s)^2} \tag{1.3}$$

The step response of the system and the relative bode plots are shown in Figure 1.9 and Figure 1.10.

The response with the current controller has the following characteristics: overshoot of 3.68 %, no steady state error and a settling time $t_s = 0.1083$ sec.

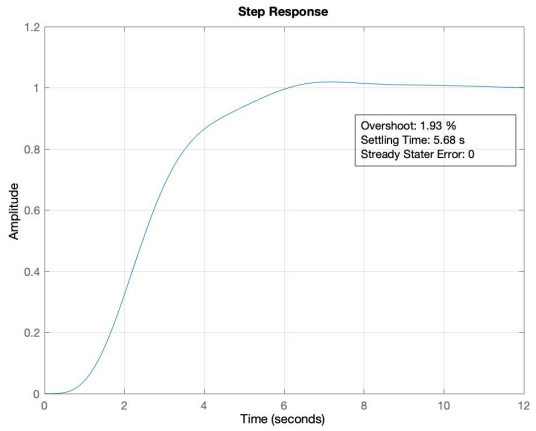

Figure 1.7: Feedback system with lead-lag controller response to a step input

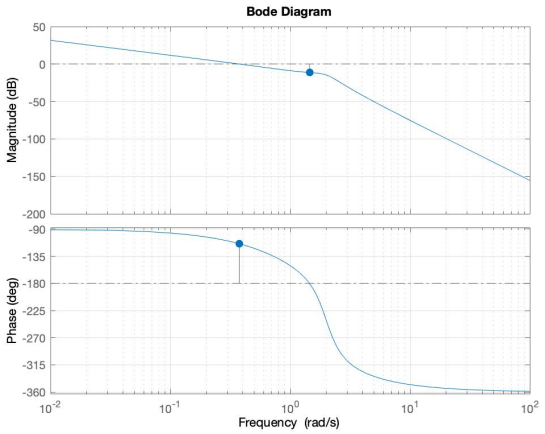

Figure 1.8: Bode plot of the system with lead-lag controller

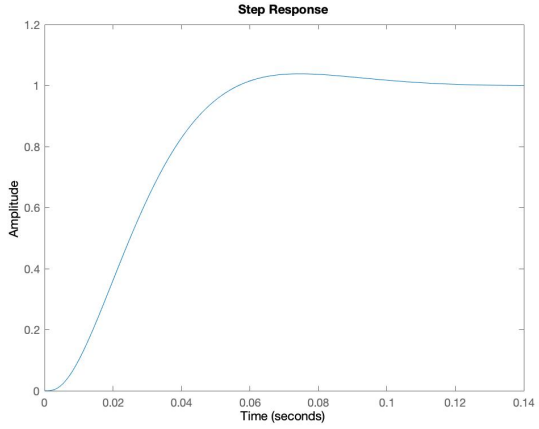

Figure 1.9: Feedback system with compensator response to a step input

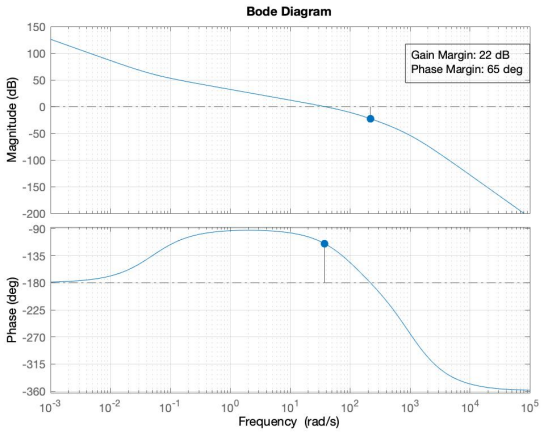

Figure 1.10: Bode plot of the system with compensator

1.2. Disturbance rejection

To attenuate disturbances the sensitivity transfer function

$$S = 1/(1+GC)$$

must be very high for low frequencies (typical for disturbances). In practice, we can use the previous controller and just increase the gain such that there is more attenuation at lower frequencies

$$C = 20\frac{100+2s}{1+0.01s}\frac{s^2+s+4}{(1+0.001s)^2} \tag{1.4}$$

This will lead though to a finite steady value of the error as can be seen in **??**. This leads though to some oscillation in the response to step in the reference signal Figure 1.13 To better understand the type of controller we need to actually drive the error to zero we analysed the steady state response to a step disturbance. Given $H_{yq} = G/(1+CG)$, it follows that

$$E = \lim_{s\longrightarrow 0} sH_{yq} \approx \lim_{s\longrightarrow 0} s\frac{1}{s^2+k_p} \tag{1.5}$$

We therefore need a pure integrator term to drive the error to zero, the new error would be

$$E = \lim_{s\longrightarrow 0} sH_{yq}\frac{1}{s} \approx \lim_{s\longrightarrow 0} \frac{1}{s^2+k_p+k_i/s} = 0 \tag{1.6}$$

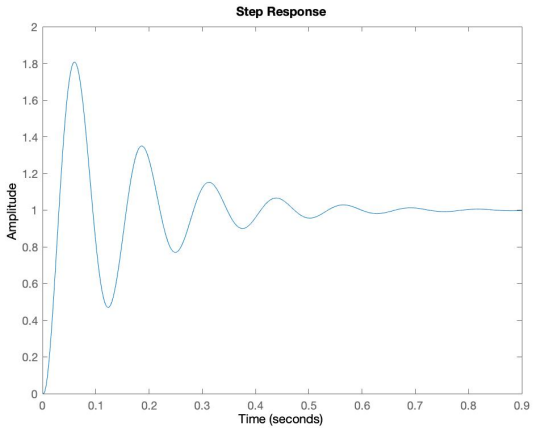

Figure 1.11: Response to a step input in the reference signal

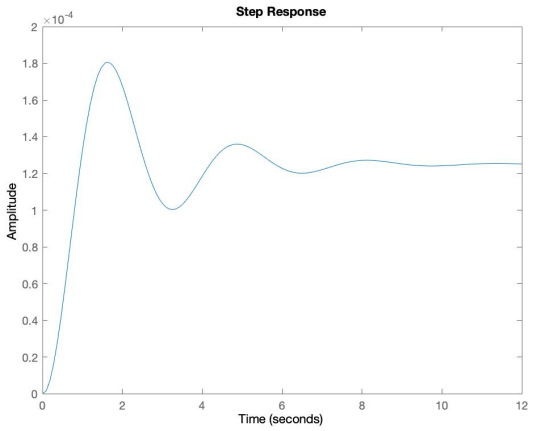

Figure 1.12: System response for a step disturbance

The controller for disturbance rejection is therefore given by

$$C = 20\frac{10+2s+\frac{10}{s}}{1+0.01s}\frac{s^2+s+4}{(1+0.001s)^2} \tag{1.7}$$

The step response of the new feedback system w.r.t a step in the reference signal and a step disturbance are shown in

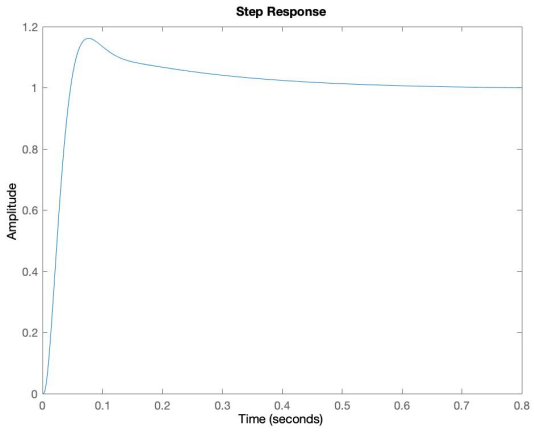

Figure 1.13: Response to a step input in the reference signal

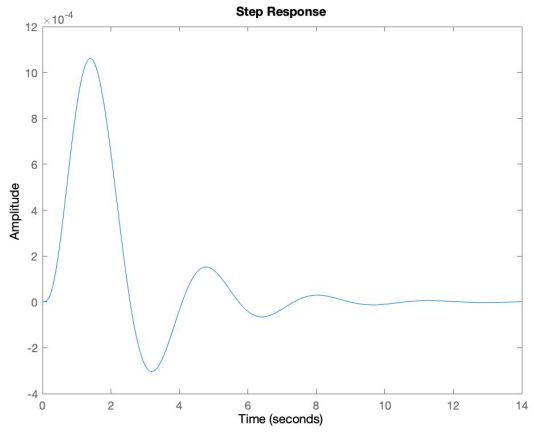

Figure 1.14: System response for a step disturbance

This last controller Equation 1.7 damps still has an initial negligible response that is totally damped in 10 seconds. The response to a step input in the reference signal presents a slightly longer settling time compared to the one related to the controller in Equation 1.3 and a higher overshoot (1.17)).

2

Discrete Controller Design

2.1. Continous state space representation

The equivalent state space formulation for the plant Equation 1 in canonical form is

$$\dot{x} = \begin{bmatrix} 1 & 2 & 0 & 0 \\ 2 & 0 & 0 & 0 \\ 0 & 1 & 0 & 0 \\ 0 & 0 & 1 & 0 \end{bmatrix} x + \begin{bmatrix} 0.5 \\ 0 \\ 0 \\ 0 \end{bmatrix} u \tag{2.1}$$

$$y = \begin{bmatrix} 0 & 0 & 0 & 1 \end{bmatrix} x \tag{2.2}$$

The state x_4 represent the altitude, x_3 the vertical velocity and x_2 proportional to the vertical acceleration. The interpretation for x_1 is more difficult but from the transfer function we can see that there is a second order system relating the position of the motors and the vertical acceleration: $(s^2 + s + 4)\ddot{Z} = M$ where M is the motor position.

2.2. Discretization

The plant has been discretized using a zero order hold with a sampling frequency twice as the cross over-frequency of the reference-track controller, which is approximately $\omega_c = 300\text{rad/s}$. Therefore the sampling period is $T_s \approx 0.0105$ s The discretized plant is given by

$$G_d(z) = \frac{5e-10z^3 + 5.489e-09z^2 + 5.477e-09z + 4.969e-10}{z^4 - 3.989z^3 + 5.968z^2 - 3.968z + 0.9896} \tag{2.3}$$

The controllers have been discretized using the same sampling frequency using the Tusting approximation. The reference track controller is given by

$$C_{rd}(z) = \frac{6.789e07z^3 - 2.029e08z^2 + 2.022e08z - 6.715e07}{z^3 + 1.046z^2 + 0.03663z - 0.1443} \tag{2.4}$$

and the disturbance rejection controller is

$$C_{dd}(z) = \frac{6.966e07z^4 - 2.743e08z^3 + 4.05e08z^2 - 2.658e08z + 6.542e07}{z^4 + 0.04588z^3 - 1.009z^2 - 0.1809z + 0.1443} \tag{2.5}$$

In Figure 2.1 are shown the the continuous and discrete system responses to step in the reference signal. Instead, Figure 2.2 are shown the continuous and discrete system responses to step disturbance.

2.3. Pole Placement

In this section, we choose the discrete pole locations of the system to set-point tracking the reference signal. The general structure of the system can be in Figure 2.3.

We chose the poles to be all real to avoid overshoot and to aim for a similar performance w.r.t. the controller treated in chapter 1. The sampling period is $T_s = 0.0056$ s ($\omega_s = 1.12$ rad/s) and the discrete poles are $p = [0.6065 0.5278 0.5134 0.4856]$. The response to the feedback system to a step input (adjusting for the dcgain) can be seen in Figure 2.4. There is no overshoot and the settling time is $T_{settle} = 0.083$ s

2.4. Dynamic Observer

In this section, we show the design of an output feedback controller with an observer.

The structure of the system with feedback and the observer is shown in Figure 2.5. The corresponding continuous poles for the observer were chosen to be $p = [-180, -230, -240, -260]$, twice in magnitude w.r.t the pole of the feedback

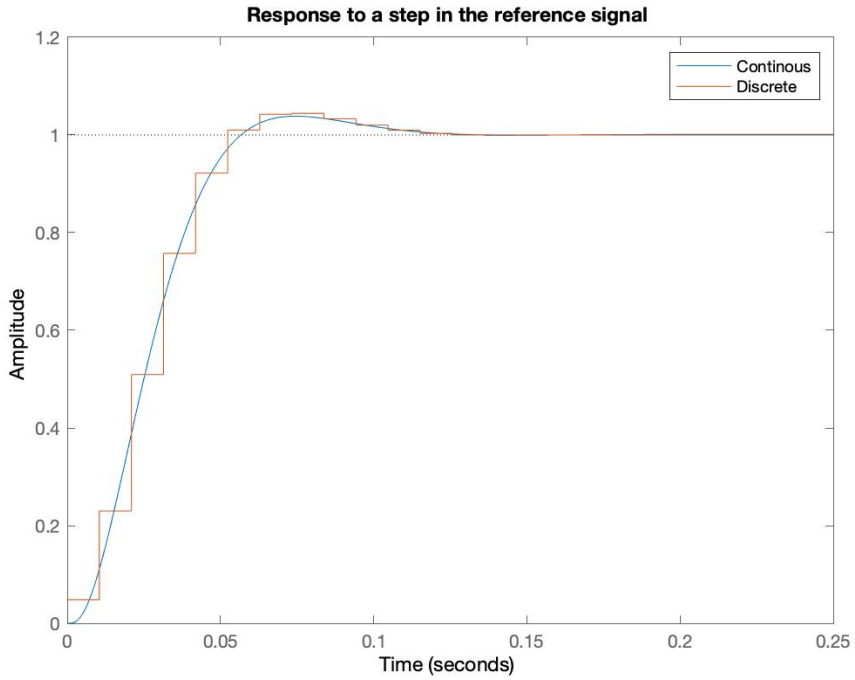

Figure 2.1: Continuous and discrete system responses to step in the reference signal

system alone. Faster poles are necessary for the observer to track the output of the feedback system. The sampling period adjusted to $\omega_s = 1.41 \times 10^3 rad/s$. The discrete poles are therefore located at $p_d = [0.6703, 0.5998, 0.5866, 0.5611]$. The poles were placed by choosing the right matrix L via pole placement on the matrices A^T and C^T.

To test that the observer is working properly we initialised the system with the initial state $x_0 = [0,0,0,2]$ which corresponds to an initial altitude of 2 m. A step function was then applied to the system. The results of the simulation are visible in Figure 2.6. The observer initially overshoots but quickly starts to track the output y and it reaches the same asymptotic value of the actual model.

We further improve the observer by ensuring that the system is able to reject disturbances via integral action. The new structure of the observer model is visible in Figure 2.7. The pole of the integration is obviously at $z = 1$ and its gain is $K_i = 10^10$. The response of the system to a disturbance of 10^6 (to compensate for the dc gain) is shown in Figure 2.8. The disturbance dies out approximately in 0.5 seconds. For this case, we chose to not change the sampling period to preserve the characteristics of the observer for the servo-tracking task.

2.5. Digital LQR controller

To perform state feedback with an LQR we have to first define the matrices Q and R which penalises respectively deviations from the reference track and the use of actuation.

We first started testing the response of the system with $Q = I$ and $R = 1$. In Figure 2.9 can be seen the simulation to a step response, the settling time is rather high, around 15 seconds.

We then proceed to modify the Q matrix to

$$Q = \begin{bmatrix} 1000 & 0 & 0 & 0 \\ 0 & 100 & 0 & 0 \\ 0 & 0 & 10 & 0 \\ 0 & 0 & 0 & 1 \end{bmatrix}$$

while keeping R = 1. The step response associated with this matrix is shown in Figure 2.10. Also, in this case, the settling time is high even if slightly reduced w.r.t the previous case. This is due to the fact the actual variable that represents height is x_4 and it should be the most penalized.

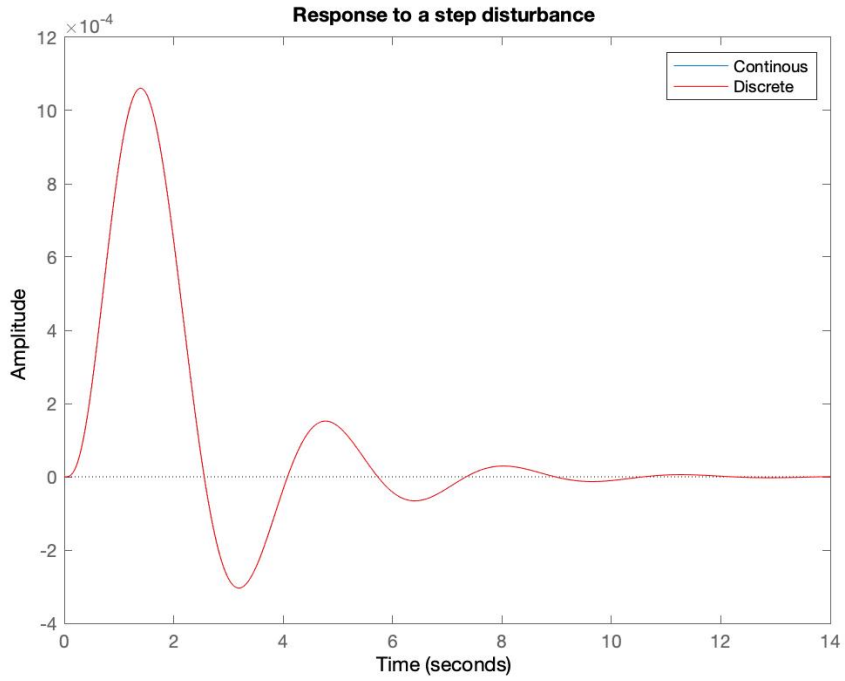

Figure 2.2: Continuous and discrete system responses to step disturbance

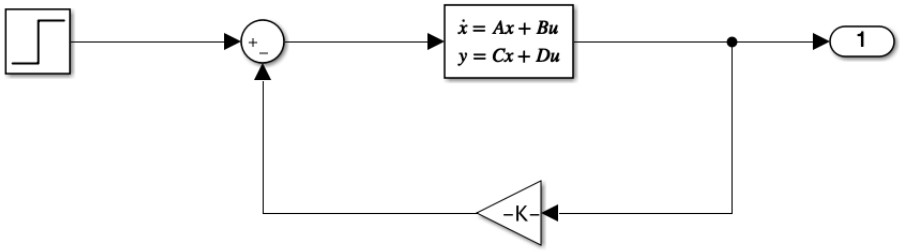

Figure 2.3: Structure of the state feedback system with pole placement

In the following case we took Q to be

$$Q = \begin{bmatrix} 1 & 0 & 0 & 0 \\ 0 & 1 & 0 & 0 \\ 0 & 0 & 100 & 0 \\ 0 & 0 & 0 & 1000 \end{bmatrix} \tag{2.6}$$

and R = 0.1, to favour higher use of the actuators. The results of this LQR controller are shown in Figure 2.11 where the setting time is 2.12 seconds with an overshoot of 2.63 %. Further increasing the value of $Q(4,4)$ or reducing R does not lead to a better performance. The sampling period for all the LQR controller is $T_s = 0.125$ sec

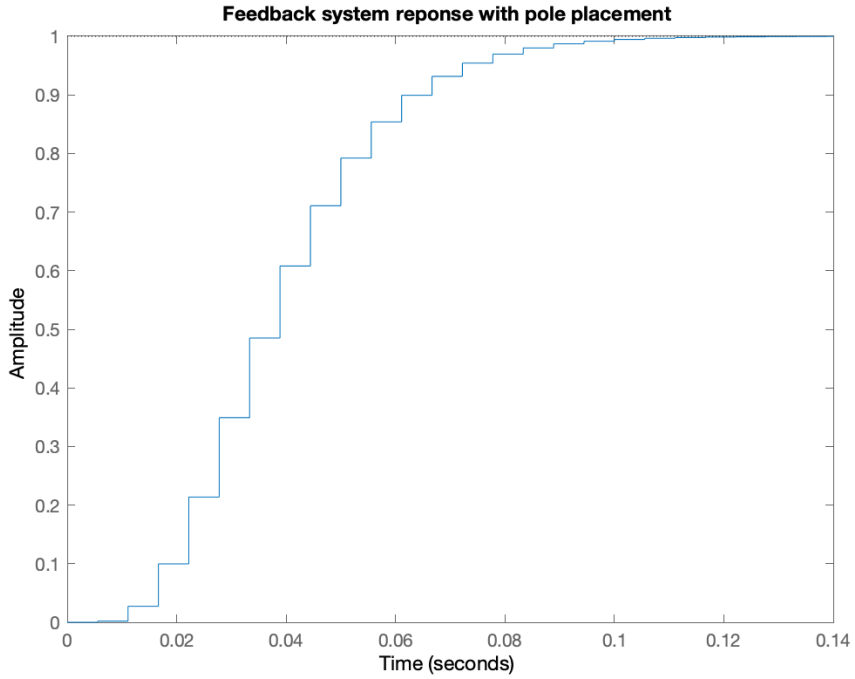

Figure 2.4: Feedback system step response

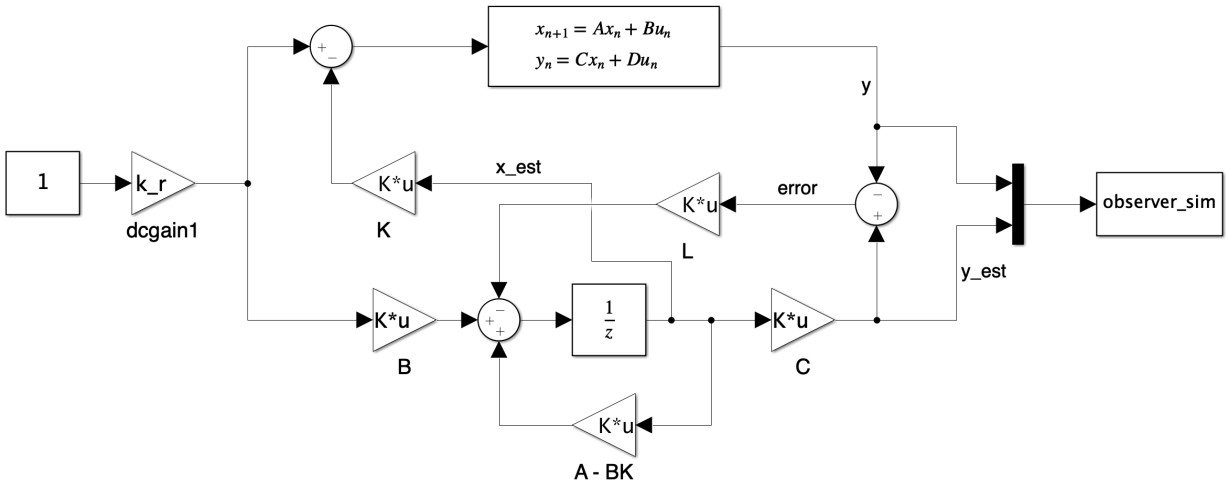

Figure 2.5: Simulink model of the observer

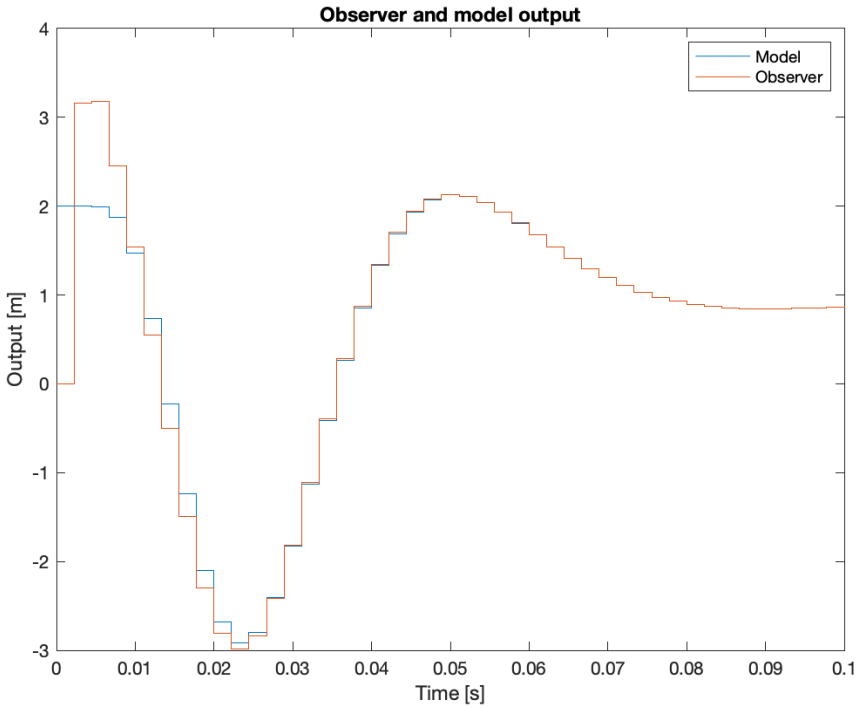

Figure 2.6: Plant output and observer output

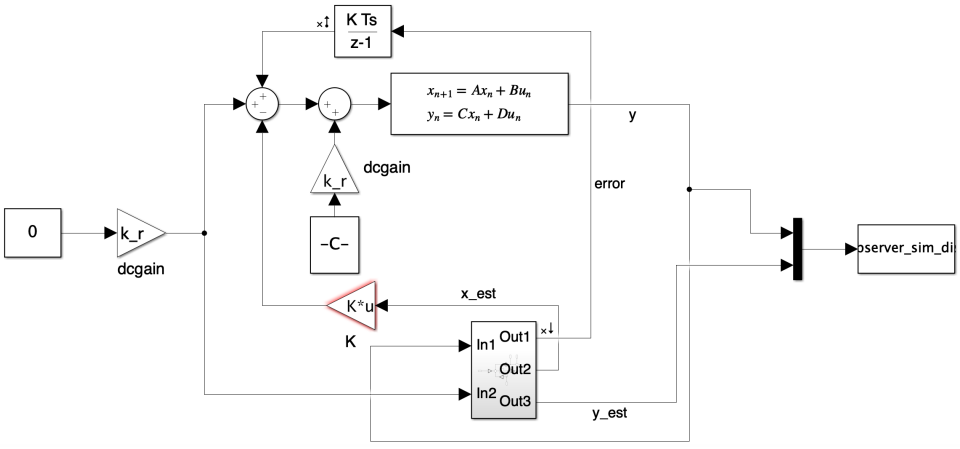

Figure 2.7: Disturbance rejection and state estimation observer

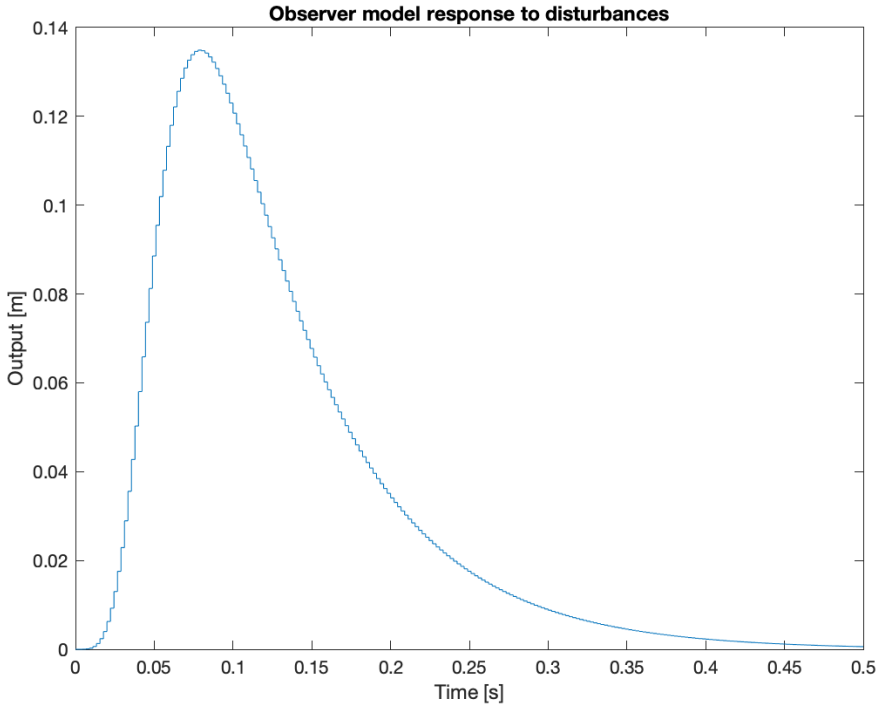

Figure 2.8: Observer system response to a disturbance

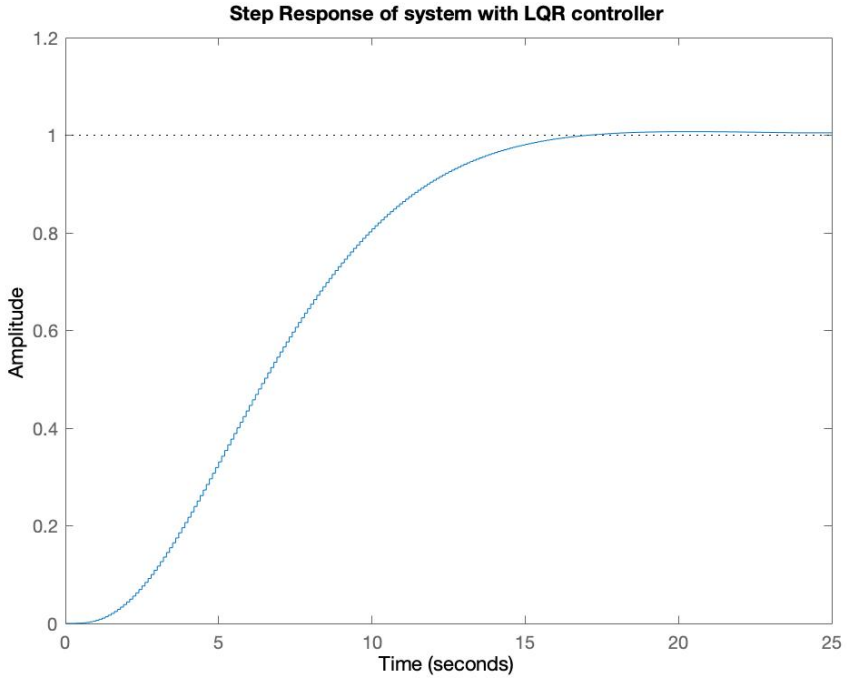

Figure 2.9: Step response of LQR controller with R = 1 and Q of **??**

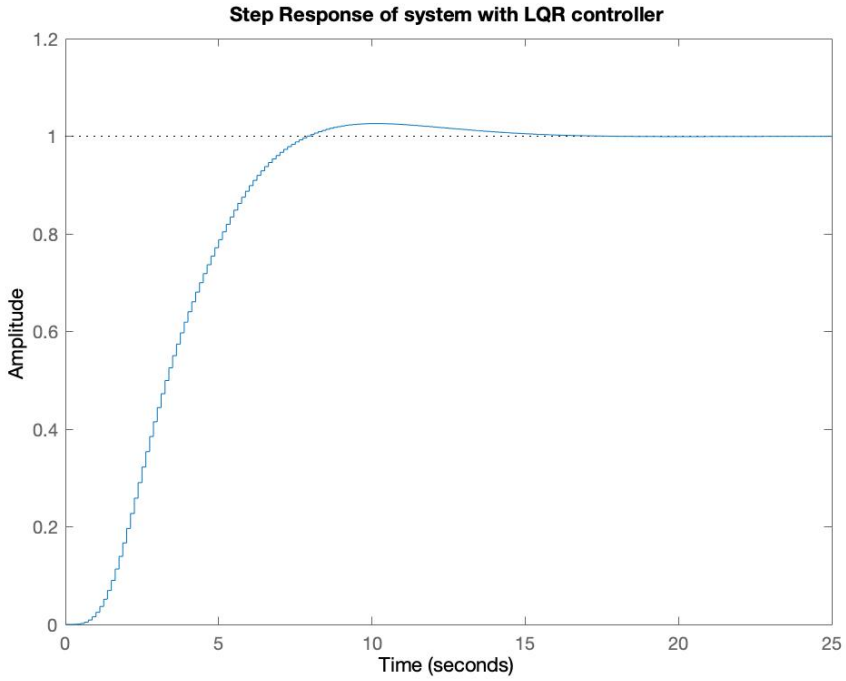

Figure 2.10: Step response of LQR controller with R = 1 and Q of Equation 4.3

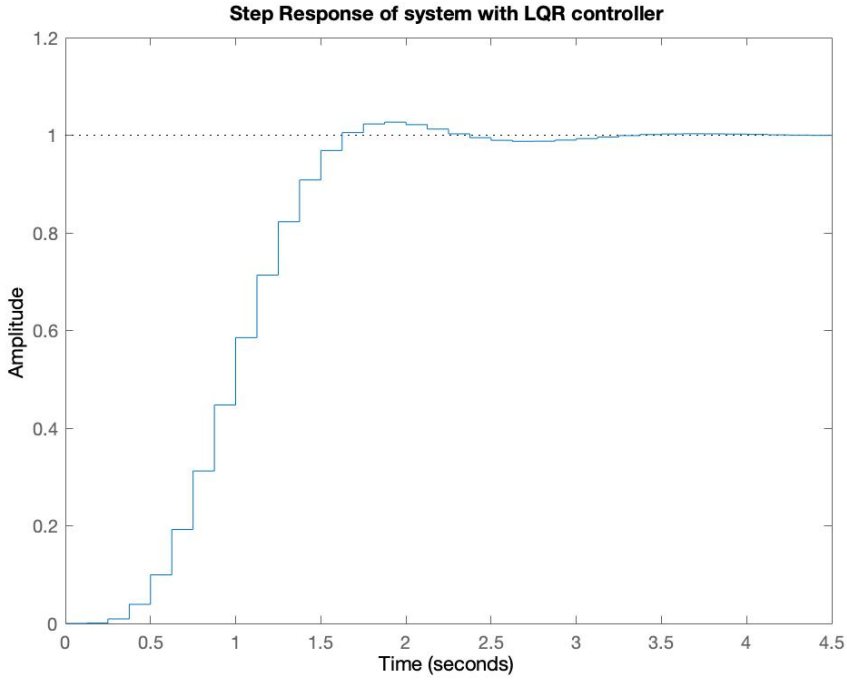

Figure 2.11: Step response of LQR controller with R = 0.1 and Q of Equation 2.6

3

Control input reduction

In this chapter, we redesigned the PID like, pole placement and LQR controllers to make sure that the actuation is not saturated by constraining the controller input to ±2.5.

3.1. PID controller

The PID like controller, discretized in chapter 2, has the continuous form

$$C_{pid} = 20\frac{10+2s+\frac{10}{s}}{1+0.01s}\frac{s^2+s+4}{(1+0.001s)^2} \tag{3.1}$$

and has its control input to a step response is shown in Figure 3.1

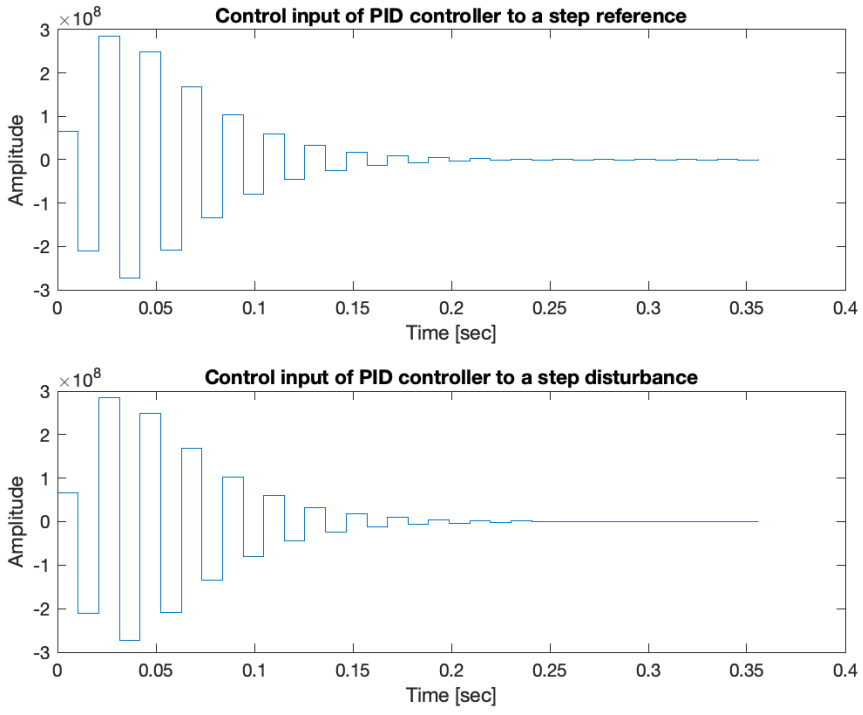

Figure 3.1: Control input of the original PID controller for a step response

The control inputs are an order of magnitude higher than it is supposed to be. To decrease it we have to drastically reduce the bandwidth of the controller. We can accomplish so by re-positioning the poles and zero of the compensator, the new controller is

$$C_{pid-new} = 3\frac{1+s+\frac{1}{s}}{1+s}\frac{s^2+0.1s+0.01}{(1+s)^2} \tag{3.2}$$

The new controller is discretized with a sampling frequency $\omega_s = 2\pi$ rad/s. The new control input for a step reference command and disturbance with the new controller is shown in Figure 3.2

As can be observed the performance is highly degraded, the system response to a step reference has an overshoot of approximately 50% and a settling time of approximately 30 sec.

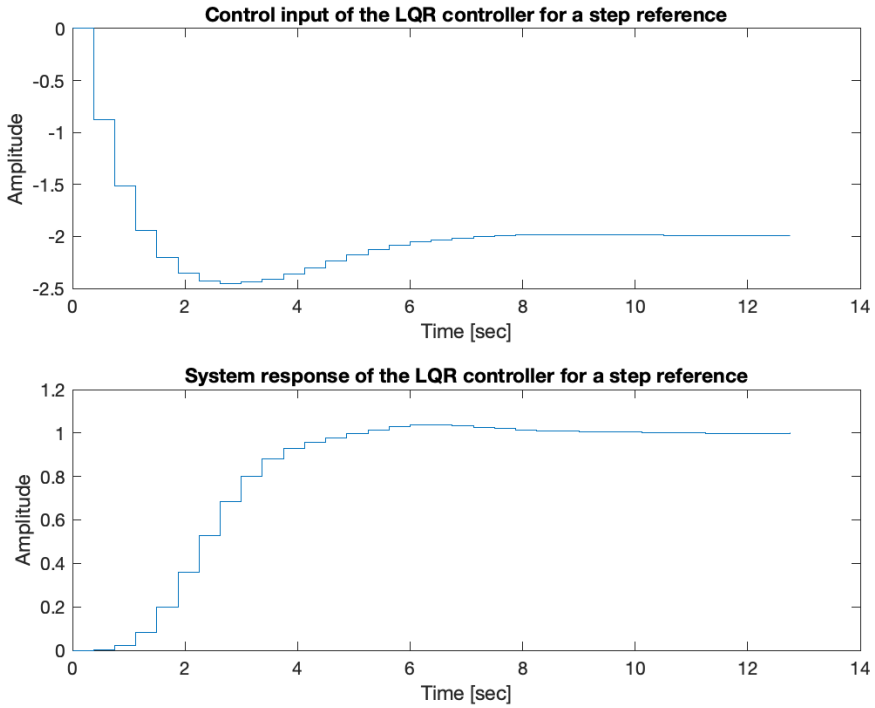

Figure 3.2: Control input of the new PID controller for a step reference and disturbance

3.2. Pole placement controller

The original system had the continuous poles at $[-90, -115, -120, -130]$ and their discrete counterpart (with sampling freq $\omega = 2.827410^3$) at [0.8187, 0.7745, 0.7659, 0.7491]. The control input for this controller is again way too high and can be seen in Figure 3.3.

To reduce the control input we moved the position of the poles. The new continuous poles are located at $p = [-1.35, -1.45, -1.50, -1.55]$, which with a sampling freq $\omega_s = 8.5$ rad/s correspond to the discrete poles $p = [0.6065, 0.5845, 0.5738, 0.5632]$. The new control input and the system response with the new controller is shown in Figure 3.4.

Performance is degraded again: the settling time is now close to $T_s = 8$ sec.

3.3. LQR controller

The original controller designed in chapter 2 gives to the plant a control input that is too high as shown in Figure 3.5.

To reduce the control input we have to reduce the weights in the Q matrix related to the states and increase the value of R to penalise high values of control inputs. For the redesigned LQR controller we choose the following matrix Q

$$Q = \begin{bmatrix} 1 & 0 & 0 & 0 \\ 0 & 1 & 0 & 0 \\ 0 & 0 & 1 & 0 \\ 0 & 0 & 0 & 100 \end{bmatrix}$$

and a value for R of

$$R = 100$$

Using a sampling frequency $\omega_s = 16.75$ rad/s we obtained the control input and the step response showed in Figure 3.6.

The settling time for the new controller raised to approximately 6 seconds.

3.4. Steady state error elimination

In this section, we described a strategy on how to eliminate steady-state errors in a robust manner for the previous controllers. The PID like controller already has an integrator that eliminated steady-state errors and therefore no further

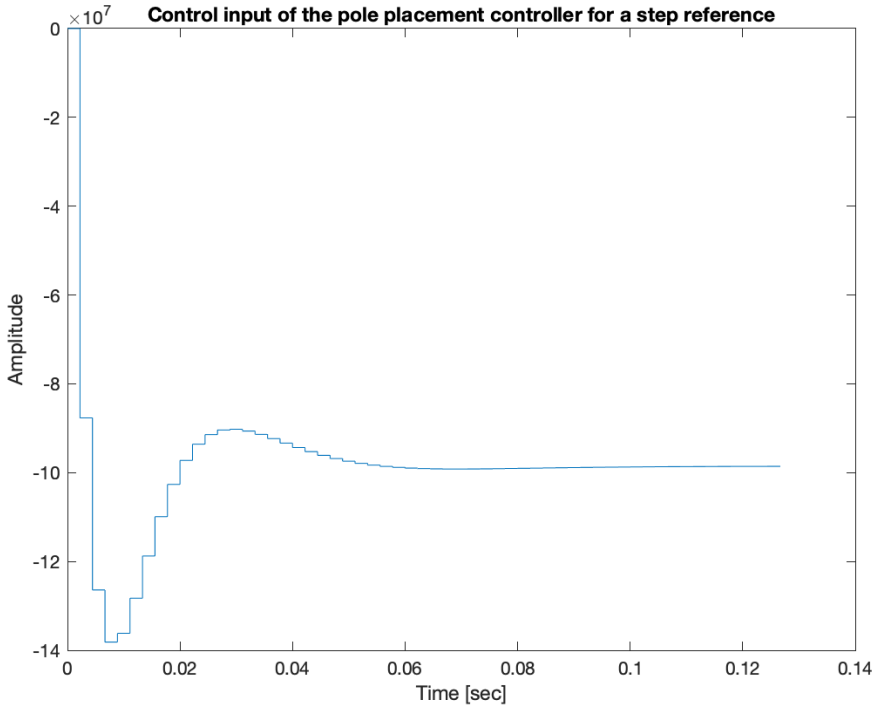

Figure 3.3: Control input of the pole placement controller for a step response

action is needed. For the pole placement and the LQR control, a feed-forward term can be applied to match the response to the desired response. The feed-forward approach though does not take into consideration the presence of load disturbances that will inevitability affect the steady-state response of the system. To counteract disturbances in full feedback state spaces we can augment the state space with an integrator. This correspond in adding a state $\dot{q} = y - r$ that is fed back. The schematics of adding the integral action to a feedback state system is shown in Figure 3.7.

This scheme can be applied both the pole placement and LQR controller since they are both state space feedback system. We consider here a modified version LQR controller developed in section 3.3 equipped with integral action augmentation. The integral action constant $k_i = 0.15$ and sampling frequency $\omega_s = 6$ rad/s the responses to a step disturbance and step reference can be seen in **??**nd **??** The system rejects the disturbance in around 30 seconds without much oscillatory behaviour. The step reference is followed exactly with a settling time of approximately 15 seconds. The system is therefore somewhat slower than the version without integral action.

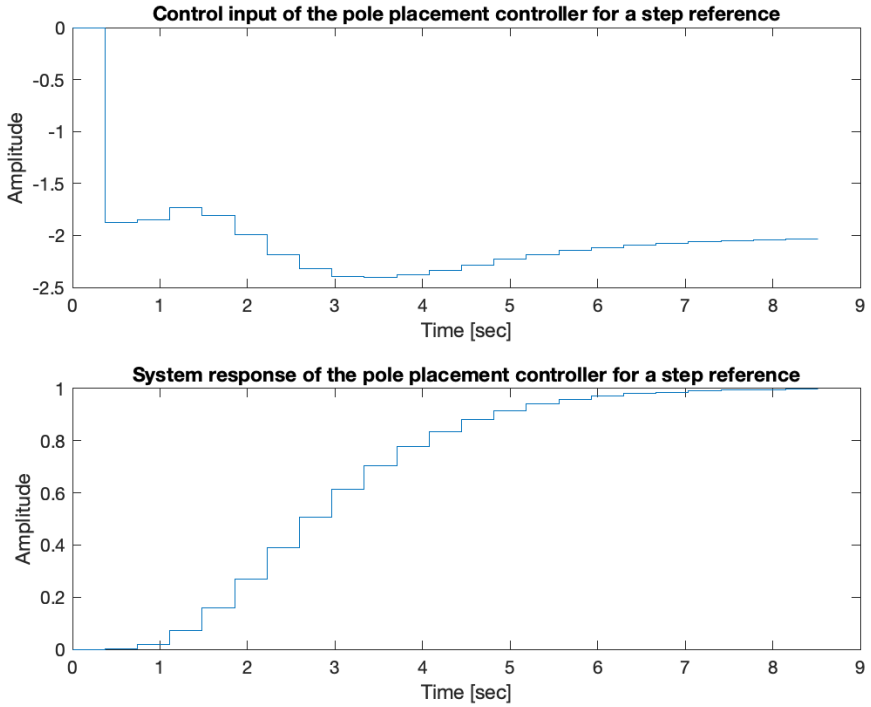

Figure 3.4: Control input of the new pole placement controller and response of the system for a step reference

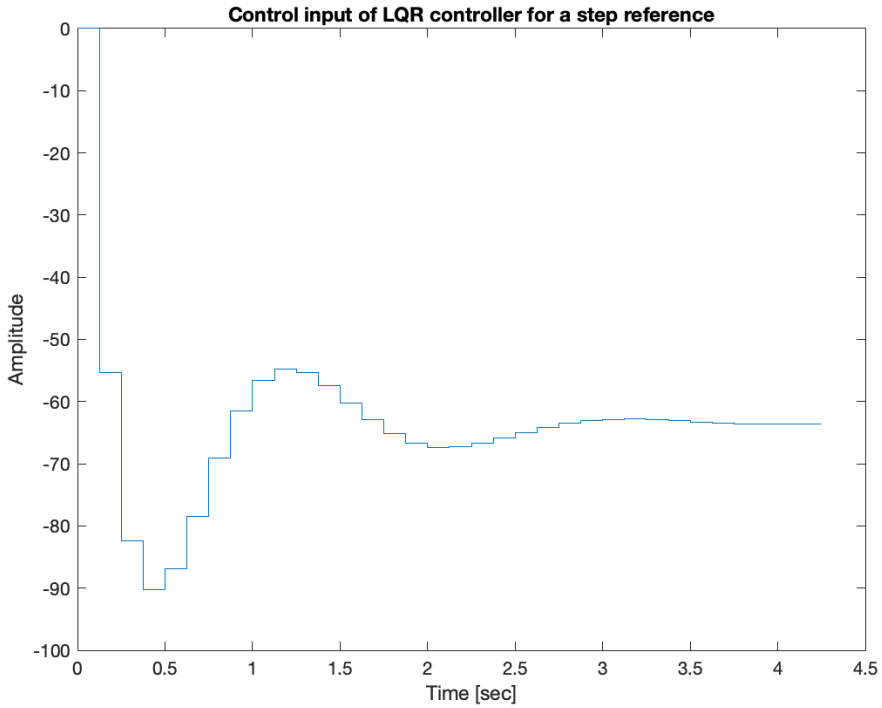

Figure 3.5: Control input of the LQR controller for a step response

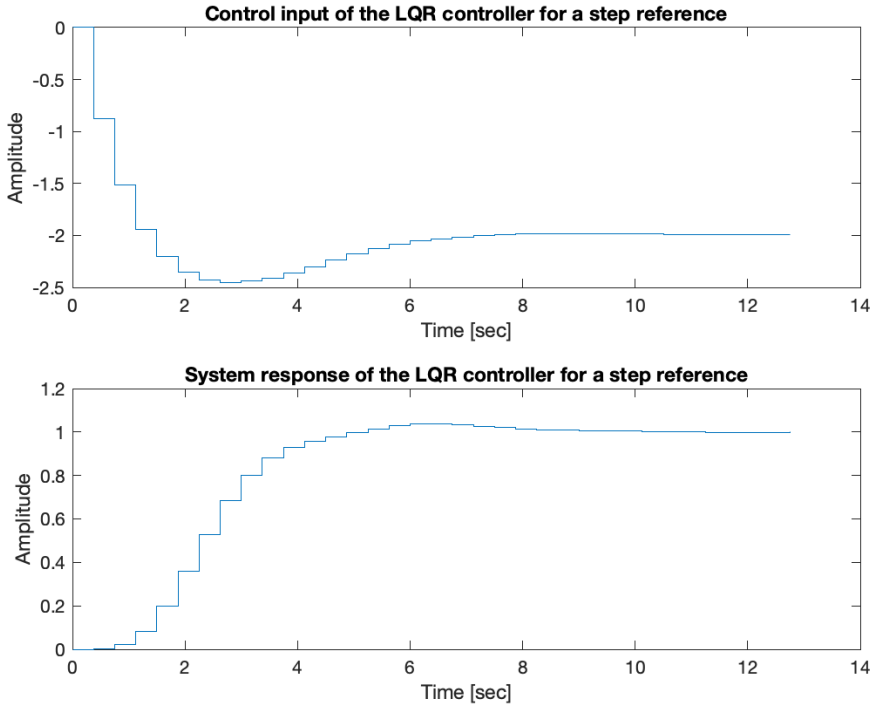

Figure 3.6: Control input of new LQR controller and system response to a step reference

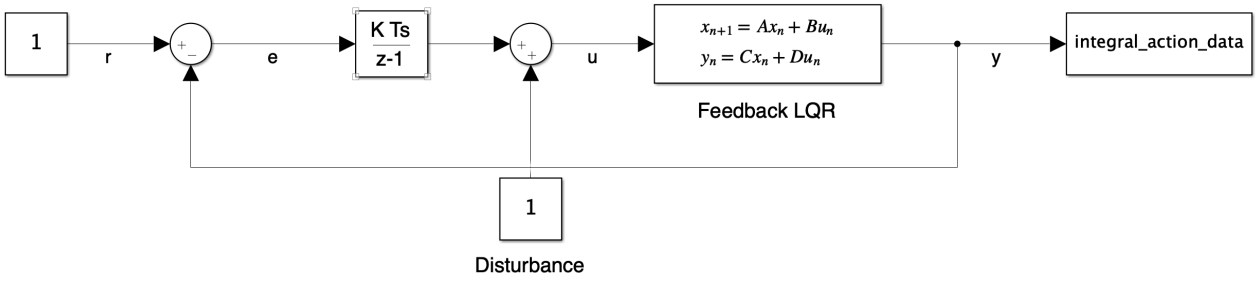

Figure 3.7: Integral action added to state feedback in Simulink

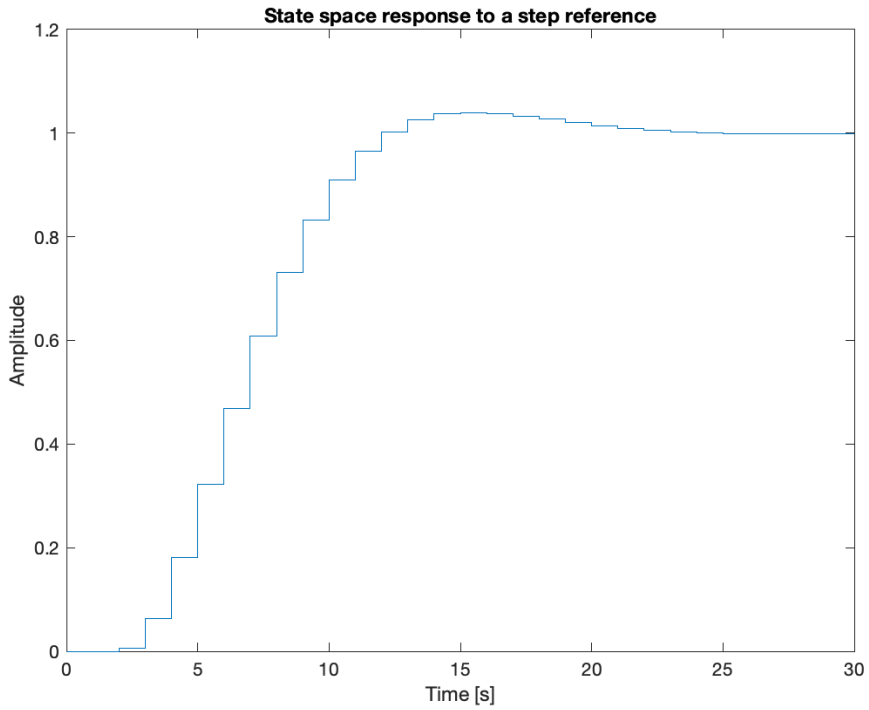

Figure 3.8: Integral action LQR system response to a step reference

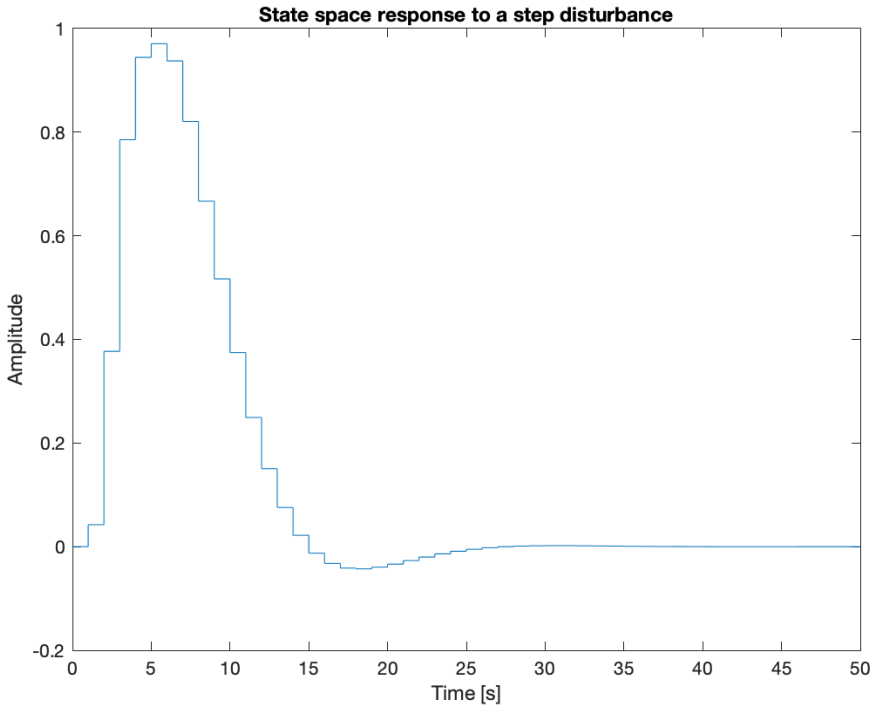

Figure 3.9: Integral action LQR system response for a step disturbance

4

Effect of delay

In this chapter, we addressed how to integrate possible delays into the controlled system and analyse their effects on the performance of the controllers. We modified the controllers developed in chapter 2 introducing delay and tuning them again to still satisfy the requirements. In general, delays decrease the phase margin of the system and to maintain stability we might have to decrease the gain of the controllers.

4.1. PID like controller delay

To introduce delay into the PID controller it is sufficient to multiply the plant discrete transfer function by the delay factor $\frac{1}{z}$. The PID controller used is shown in Equation 1.4. The sampling frequency for both the normal and delayed system is $\omega_s = 600$ rad/s. The response for both systems to a step input is shown in Figure 4.1.

We can see that the delayed system has a much higher overshoot and less damped behaviour. To regain the phase margin we halved the gain of the controller resulting in

$$C = 20\frac{100+2s}{1+0.01s}\frac{s^2+s+4}{(1+0.001s)^2} \tag{4.1}$$

The new system responses are shown in Figure 4.2. Now both the system comply with the original requirements.

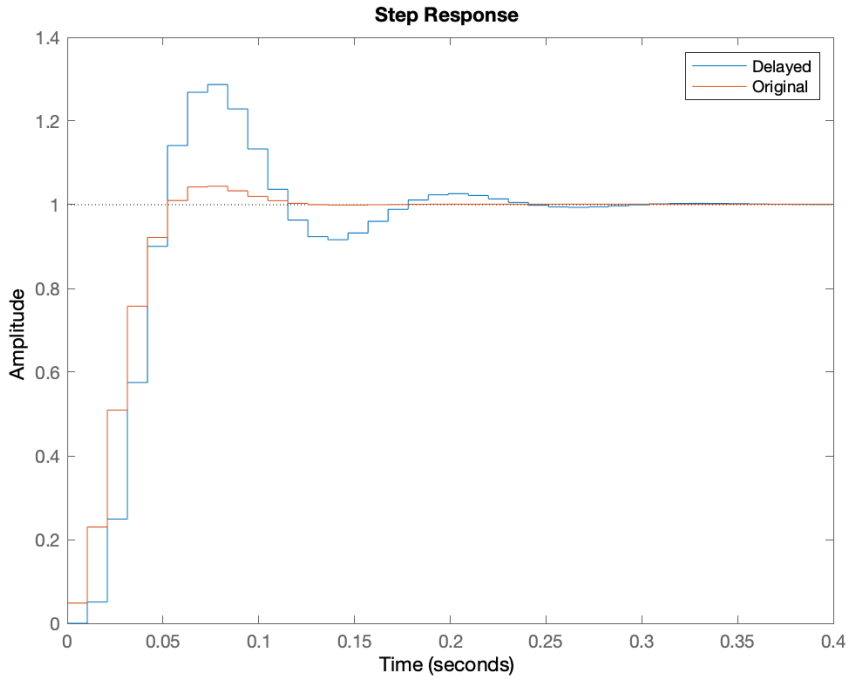

Figure 4.1: Step response of the original controller and the delayed controller

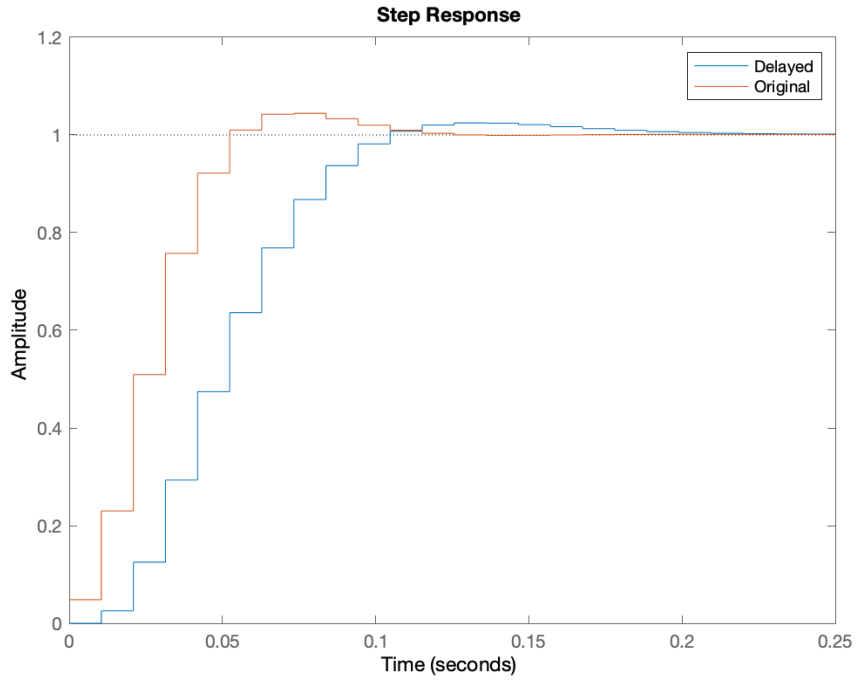

Figure 4.2: Step response of the original controller and the updated delayed controller

4.2. Pole placement controller with delay

The controller's poles used for this task are shown in section 2.3. Delay can be introduced into the state space by augmenting the system as follows

$$\begin{bmatrix} x(k) \\ u(k) \end{bmatrix} = \begin{bmatrix} \Phi & \Gamma \\ 0 & 0 \end{bmatrix} \begin{bmatrix} x(k-1) \\ u(k-1) \end{bmatrix} + \begin{bmatrix} 0 \\ 1 \end{bmatrix} u(k-1) \tag{4.2}$$

or in Simulink can be implemented as shown in Figure 4.3, which also includes integral action.

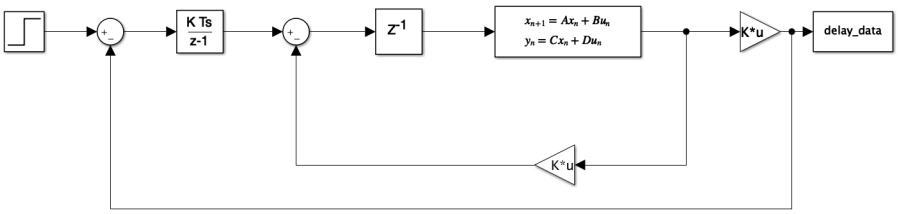

Figure 4.3: Simulink model of delayed state space model with integral action

For the following simulation, we used the Simulink model. For a sampling frequency of $\omega_s = 2260$ rad/s the responses of both systems are shown in Figure 4.5. It can be seen that the delayed model is already unstable and that we need to redesign it.

The integral gain of the controller has been lowered from $k_{i0} = 10^9$ to $k_{i1} = 2 \times 10^8$ and the its corresponding continuous poles are $p = [-63, -80, -84, -91]$ lower than the original ones $p_0 = [-90, -115, -120, -130]$. The response of the new system in shown in **??**. Now both controller meet the requirements.

The sampling frequency for this system has been chosen higher than usual because the performance of even the non-delayed controlled degraded quickly with a decrease in the sampling frequency.

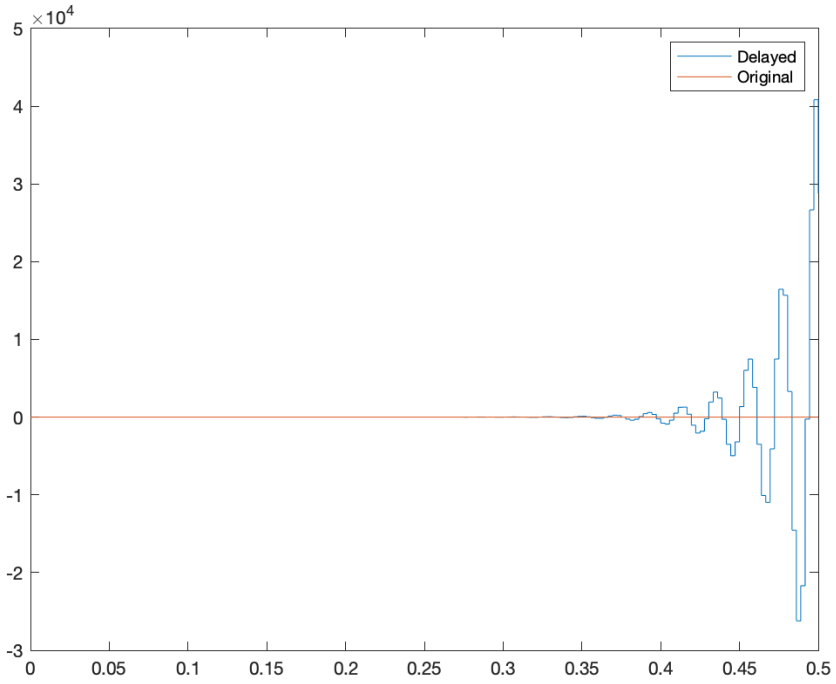

Figure 4.4: System response (pole placement) for a step reference

4.3. LQR controller with delay

The LQR controller used for this section has the same Q and R matrices of the controller presented in Equation 2.6. The structure of the controller is shown in Figure 4.6.

The responses of the original system and the delayed one are shown in Figure 4.7, the sampling frequency is $\omega_s = 50$ rad/s. The delayed system is unstable and we have to redesign it. The feedforward term k_r has been lowered from 30 to 9, the integral gain k_i has been lowered from 30 to 9 and the new Q matrix is

$$Q = \begin{bmatrix} 1 & 0 & 0 & 0 \\ 0 & 1 & 0 & 0 \\ 0 & 0 & 10 & 0 \\ 0 & 0 & 0 & 100 \end{bmatrix} \tag{4.3}$$

The new responses to a step reference are shown in Figure 4.8. Now both controllers satisfy the requirements.

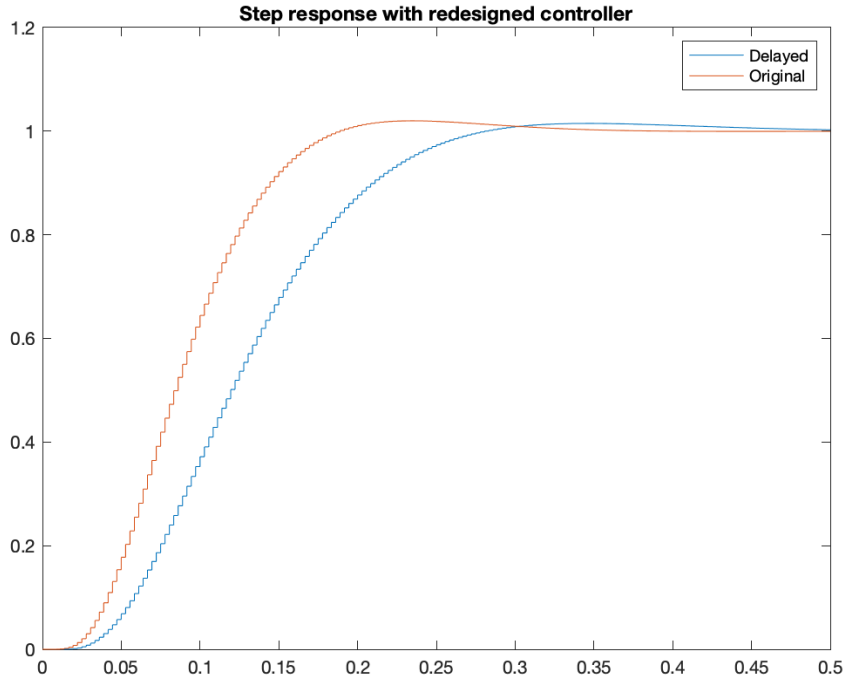

Figure 4.5: System response (pole placement) with new controller for a step reference

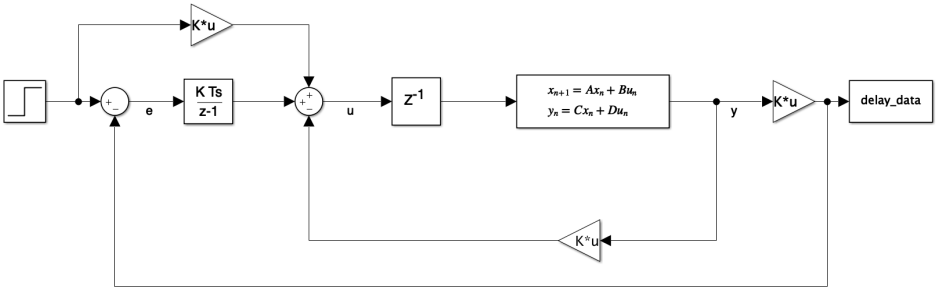

Figure 4.6: System response for a step reference

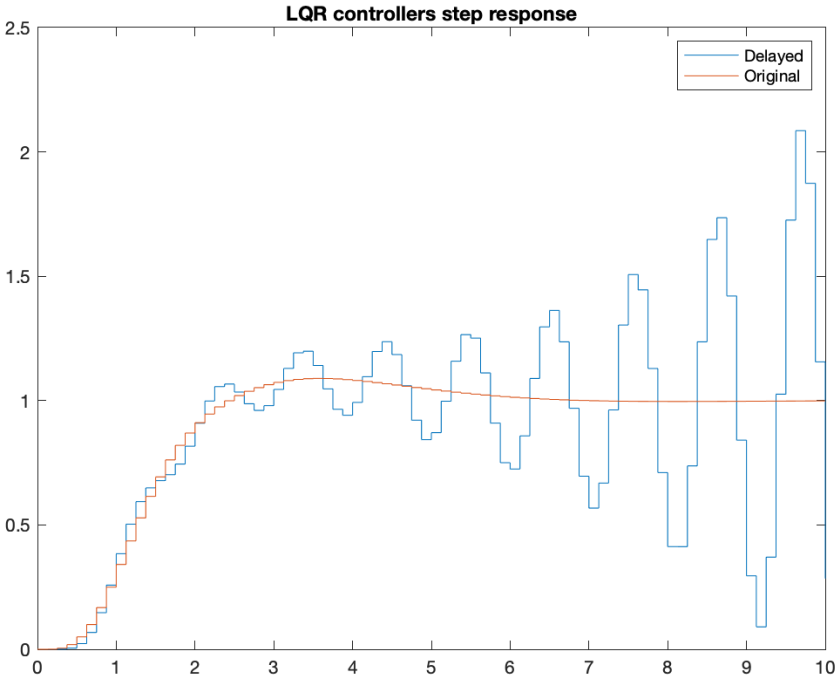

Figure 4.7: LQR system response for a step reference

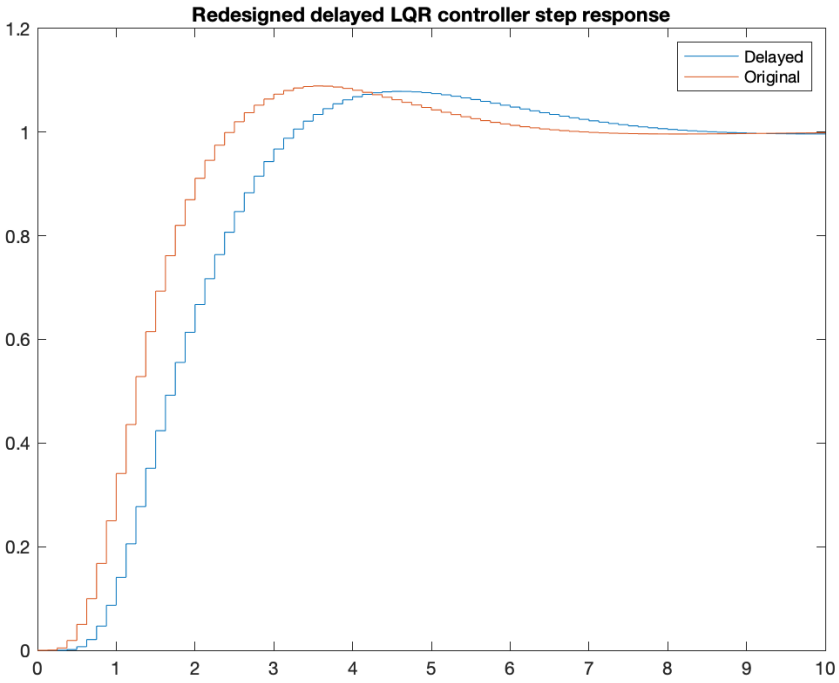

Figure 4.8: LQR redesigned system response for a step reference

5

Conclusions

In this report we designed several controller for a VTOL aircraft.

In chapter 1 we designed two continuous controllers, one for servo-tracking and the other tuned for disturbance rejection. Both servos try to minimize settling time, have a zero steady state error and an overshoot less than 5 %.

The two controllers are discretized in chapter 2 by appropriately choosing a discretization scheme. Furthermore in chapter 2 we designed a pole placement controller and equipped it with an observer to output-feedback controller. Furthermore we designed an digital LQR controller for reference tracking.

In chapter 3 we revised the design of the controllers to make sure that the output of the controllers was in magnitude below 2.5 to avoid saturation of the actuators. At the end of the chapter integral action was introduced as way to generate a robust reference tracking state feedback system.

In chapter 4 we analysed the effects of delays in the control system, which often result unstable, and redesigned them to meet the original requirements.